1

Lung Depth Dose from Inhalation of ^{222}Rn Progeny

A. Mohamed, M.Abd El-Hady, Mona Moustafa, M. Yuness and M.M. Ismail[*]
Physics Department, Faculty of Science, Al Minea University, Al Minea and [*]*Physics Department, Faculty of Science, Al Azhar University, Cairo, Egypt.*

IN THE CASE of internally deposited radionuclides, direct measurement of the energy absorbed from ionizing radiation emitted by the decaying of these *radionuclides* is rarely, if ever, possible. Therefore, one must rely on *dosimetric models* to obtain estimates of the spatial and temporal patterns of energy deposition in human lung. These models always require information about the parameters of activity size distributions of *radon progeny*. In the present work, the attached and unattached activity size distribution of ^{222}Rn progeny (^{214}Bi and ^{214}Po) were measured in indoor air of Minia University, Minia, Egypt. The attached fraction was collected using a low-pressure Berner cascade-impactor technique. A constructed wire screen diffusion battery was used for collecting the unattached fraction. Most of the attached activities for ^{214}Bi progeny were associated with the *aerosol particles* of the accumulation mode. The AMAD of this mode for ^{214}Bi was determined to be 350 nm with GSD of 3. The GSD of unattached size distributions for ^{214}Po is 1.29 with AMTD of 1.25 nm. An analytical method has been developed to compute the local energy deposition of ^{214}Po alpha particles in a target volume of 1 μm spheres located at different depths in bronchial epithelium. In order to reach the target, alpha particles travel either through tissue alone or through air and tissue. While the depth-dose distributions in the case of nuclides uniformly distributed within the epithelium were practically constant with depth, they decreased in an almost linear fashion with increasing depth in the case of nuclides on the airway surface.

Keywords: Radionuclides, Dosimetricmodels, Radon progeny, Aerosol particles.

Doses produced by naturally occurring radionuclides are mostly caused by tissue irradiation from inhaled short-lived radon progeny (^{218}Po, ^{214}Pb, ^{214}Bi and ^{214}Po). Averaged over the whole world, about a half the annual effective dose received by a member of the general public from all natural radioactive sources, is due to inhalation of short-lived radon progeny present in indoor and outdoor air[1, 2].

The radon progeny are initially positively charged and therefore react quickly with air molecules and water vapor then form clusters with an activity median diameter (AMD) of less than 10 nm. These clusters, also called unattached radon

Emails: amermohamed 6 @ hotmail.com and D_M_YP_H @ yahoo.com

progeny ,may remain charged or be neutralized by electron scavenging by OH radicals, recombination with small ions, and charge transfer with molecules of lower ionization potential[2, 3]. They are partly deposited on surfaces, or attach to particulates present in air forming radioactive aerosols with AMD in the range of 100–2000 nm. This fraction is called attached radon progeny, to distinguish it from the unattached fraction, f_{un}. Because of deposition, radioactive equilibrium between radon and its short-lived progeny is practically never reached, and is measured with the so-called equilibrium factor, F.

The activity size distribution of radon progeny is important for evaluating the absorbed dose through the human lung. This distribution has been determined by tagging natural aerosol particles with radon progeny. However, some measurements for attached and unattached activity size distributions of ^{222}Rn progeny have been performed in the indoor air under realistic natural conditions[4-17]. Most of the observed data have shown that the size distribution of radon progeny consists of ultrafine clusters with median diameters below 4 nm (unattached activity) and progenies associated with ambient aerosol particles in sizes ranging between 100 and 1000 nm (attached activity).

The unattached fraction is deposited completely in the respiratory tract during inhalation, whereas 80 percent of the attached are exhaled without deposition[9,18,19]. The amount of unattached activities up to about 10 percent of the total activity in the air, but is considered to yield about 50 percent of the total radiation dose[9,14,20]. Therefore, it is necessary to determine the size of the unattached fraction of radon progeny [7,11,13,18,21].

Inhaled radon progeny are deposited in different regions of the human bronchial tree as functions of particle size, flow rate and flow dynamics. Following deposition and mucocillary clearance, the sensitive bronchial basal and secretory cells are irradiated by two different particle sources: i) Radon progeny in the sol and /or gel phase of the mucous layer and ii) Radon progeny within the bronchial epithelium.

In the case of internally deposited radionuclides, direct measurement of the energy absorbed from ionizing radiation emitted by the decaying radionuclides is rarely, if ever, possible. Therefore, one must rely on dosimetric models to obtain estimates of the spatial and temporal patterns of energy deposition in human lung. There are increasing demands to obtain a definitive explanation of the role of alpha particles emitted from radon progeny in the induction of lung cancer. Various authors have attempted to evaluate the dose to the respiratory tract due to the inhalation of radon progeny [22-28].

The basal and secretory cells are commonly considered as the principal target cells for alpha particle irradiation[29] though cycling cells may play an important role in subsequent tumor promotion[30]. However, no information about their relative sensitivities to malignant transformation has been reported; thus, it is

practice to assume equal radio sensitivity with respect to carcinogenesis. Basal and secretory cell nuclei are nonuniformly distributed across the bronchial epithelium and differ in their respective volumetric densities in bronchial airway generations [31,32]. The location and volumetric densities of these cells, provided by Mercer *et al.*[32] are used in the present work to evaluate cell specific doses.

For the calculation of the absorbed dose in the human lung we rely on different dosimetric models, which always need information about the parameters of activity size distributions of radon progeny in the air. Therefore, the first aim of the present study is to summarize the measured data on attached and unattached activity size distributions of radon progeny in indoor air of Minia University, Minia, Egypt. In addition, an analytical method has been developed to evaluate the absorbed dose (nGy) for a surface activity of $1 Bq/m^2$ deposited by radon progeny alpha particles in one micrometer spheres located at different depths in the bronchial epithelium.

Experimental Methods and Data Evaluation

In the present work, a low pressure Berner cascade impactor was used to determine the activity size distribution of attached progeny. The impactor consisted of eight size fractionating stages and a back-up filter holder. It operated at a flow rate of $1.7 m^3 h^{-1}$. Aluminum foils were used as collection media and a glass fiber filter as the backup filter[33]. Efficiency curves and inter stage losses of the impactor stages were determined with aerosol particles in the diameter size range of 70-6000 nm[6]. The measured 50% cut-off diameters were 82, 157, 270, 650, 1100, 2350, 4250 and 5960 nm. The total inter-stage losses of aerosol particles were less than 2% of the total activity[6].
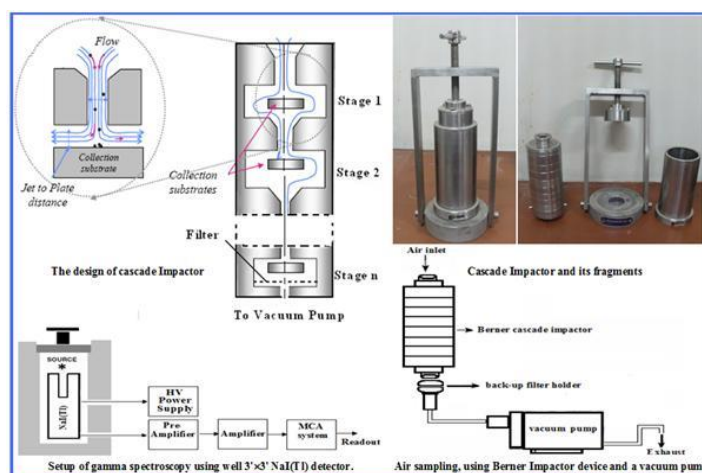

Fig. 1. Air sampling, using Berner impactor, vacuum pump and setup of gamma spectroscopy.

Several runs were conducted, using low-pressure Berner impactor, to determine the attached activity size distribution of [214]Bi. After air sampling (2h), the foils were pressed into pellets and the relative gross γ-ray emitting activities on each impactor stage were measured with a 5×5 inch NaI (Tl) detector connected to a multichannel analyzer.

The parameters of the attached activity size distribution (active median aerodynamic diameter, AMAD and geometric standard deviation GSM) were obtained using lognormal distribution method[34].

$$\ln(AMD) = \frac{\Sigma n_i \ln d_i}{\Sigma n_i}$$

$$\ln(GSD) = \left[\frac{\Sigma n_i (\ln d_i - \ln AMD)^2}{\Sigma n_i}\right]^{\frac{1}{2}}$$

(1)

where n_i and d_i are the measured fraction and the cut-off diameter in the stage i, respectively. Also, these parameters can be obtained by a graphical cumulative method. The cumulative attached activities were plotted versus the cut-off diameter of the impactor stages. The AMAD is defined as the diameter at 50% cumulative fractions. The GSD of the size distribution is defined as the diameter at 84% cumulative activity divided by the diameter obtained at 50%.

A wire screen diffusion battery was constructed to determine the size distribution of unattached radon progeny. The diffusion battery consisted of four stainless-steel screens with 24, 35, 50 and 200 mesh numbers and operated at a flow rate of 0.36 m^3 h^{-1}. The screens were calibrated with monodisperse silver aerosol particles under laboratory conditions. The measured 50% cut-off diameters of the screens were 0.9, 1.3, 1.9 and 4.0 nm. The sampler could detect 0.5 mBq m^{-3} within a 2 hr counting time with 25% statistical uncertainty.
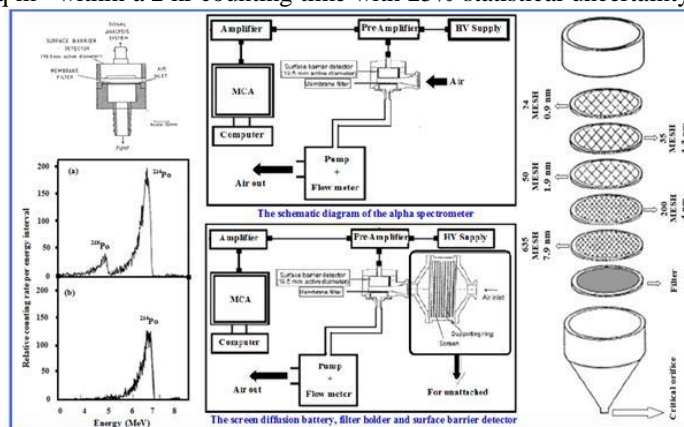

Fig. 2. The screen diffusion battery, filter holder and surface barrier detector arrangement for the measurements of the unattached fractions of radon progeny.

To determine the unattached activity fraction of ^{214}Po, the attached aerosol and total progeny fraction concentrations were measured. Each measurement consisted of two parallel samples: one with a single screen and the other as a reference sample without screen. This procedure was repeated with different screens. The screen was used for collecting the unattached activities. The activities penetrating the screen (mostly attached to aerosol fraction) and that of the reference sample were collected on membrane filters. The alpha activities were detected during and after air sampling by a surface barrier detector. According to the Ruffle[35] method, and by utilizing ^{241}Am as a radioactive source of alpha radiation, the counting efficiency of the detector was determined to be $17.0 \pm 0.5\%$. The detector has an active area of 300 mm^2 and the separation between the filter and detector is 6 mm. In order to determine the activity concentrations, measurements were performed in two steps. First, the alpha particle spectrum was collected during a sampling period of 30 min. Secondly, after waiting for a time period of 30 min without sampling, the alpha particle spectrum was measured again (during decay) for a time period of 30 min. The activity concentrations could be calculated according to a method described by Wicke[36]. The attached activities were derived from the filter sample obtained with the screen. The collected unattached activity on the screen is the difference between the measurements of the filter for the reference sample (without screen) and the screen sample.

The parameters of unattached size distribution (active median thermodynamic diameter, AMTD and GSD) were obtained from a graphical cumulative method. The cumulative unattached activity was plotted versus the cut-off diameter of the screens. The AMTD is defined as the diameter at 50% of the cumulative plot. The GSD of the size distribution is defined as the diameter at 84% cumulative activity divided by the diameter obtained at 50%.

Indoor activity size distribution of ^{214}Bi and ^{214}Po

Several attached and unattached activity size distributions (thirty samples have been performed for attached and unattached fraction) were carried out in indoor air of Minia University in the third floor. The parameters of attached and unattached activity size distributions (AMAD, AMTD and GSD) for ^{214}Bi and ^{214}Po are summarized in Table 1. In the same way, Fig. 3 shows the activity size distribution of attached^{214}Bi and unattached ^{214}Po. Because the measurements were performed at different times, considerable fluctuations in the size distributions were observed. Also, depending on meteorological conditions very low activities in the coarse mode (aerosol size range > 2000 nm) were sometimes measured. Most of the derived attached activity size distributions could be approximated as unimodal log-normal distributions represented by the accumulation mode (100 nm < aerosol particle size < 2000 nm), while the others could be approximated as bimodal log-normal distributions (accumulation and coarse mode). This might be traced to the removal processes of the particles from the atmospheres, which are controlled by dry deposition. The deposition velocity of particle in the accumulation mode was about 10^{-2} cm s^{-1}[37]. Particles

with such deposition velocities were very slowly removed and therefore their residence times were relatively long. The deposition velocity of particles in the coarse mode extended to 20 cm s^{-1} [37] and it was very high in comparison with that of accumulation mode particles. Therefore, the residence time of the particles in the coarse mode was very short and it is less likely that these particles would coagulate to produce a broad size distribution of the coarse mode. The AMAD of ^{214}Bi was calculated to be 350 nm with relative geometric standard deviation of 3.
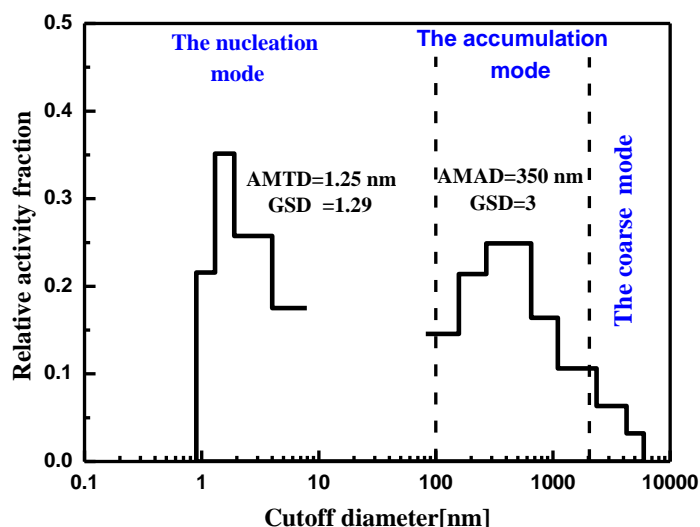

Fig. 3. **Average calculated activity size distribution of attached and unattached radon progeny (^{214}Bi and ^{214}Po) measured in indoor air with low pressure Berner cascade impactor and diffusion battery. The relative activities are plotted vs the cut-off diameter (the number of measurements is 30).**

TABLE 1. **Calculated values of active median aerodynamic diameter (AMAD), active median thermodynamic diameter (AMTD) and relative geometric standard deviation (GSD) of radon progeny (^{214}Bi and ^{214}Po) size distribution measured indoor air with a Berner impactor (BI) and diffusion battery (DB). Extreme values of measurements are given in parenthesis.**

BI			DB		
Nuclide	AMAD (nm)	GSD	Nuclide	AMTD (nm)	GSD
^{214}Bi	350 (253 -427)	3 (2.58-3.59)	^{214}Po	1.25 (1.06-1.47)	1.29 (1.19-1.37)

With the Berner impactor,[5] measured the mean activity median aerodynamic diameter of 200–500 nm for ^{214}Bi in indoor air. Yamasaki *et al.*, in Kyoto University, Japan have published an indoor size distribution of radon progeny

with mean activity median aerodynamic diameter of 255 nm with GSD 1.59. Kranrod[16] have been measured the activity size distribution of the attached radon progeny by a Micro Orifice Uniform Deposit impactor (Model 110 MOUDITM, USA) in Okinawa. The AMAD was observed 267 nm with a range from 234 to 308 and a GSD of 1.7 (range 1.6 and 1.9) which is smaller than our present value Mishra et al. [17] have been measured the activity size distribution of the attached aerosols by a developed low pressure cascade impactor. The AMAD was obtained to be 150 nm with GSD of 2.7, which is a factor of two smaller than the present value. The difference in literature values may be due to the difference of dimensions of rooms and ventilation rate in addition to may be attributed to the difference in the sampling locations.

The obtained parameters of unattached size distribution of ^{214}Po (AMTD, GSD) are also listed in Table1. The active median thermodynamic diameter of unattached fraction, AMTD, of ^{214}Po was determined to be 1.25 nm with relative geometric standard deviation of 1.29.

The present AMTD (1.25 nm) is considered to be relatively higher than the values obtained (around 0.8 nm) by Huet et al. [11] and VauPotic & Kobal[13].

Estimation of absorbed dose through out the lung

Consistent with the compartmentalization of the tracheobronchial tree with respect to the clearance pathways of deposited radionnuclides in bronchial airway generations[38] radon progeny can be found in the gel phase of the mucous layer, in the underlying sol phase and within the bronchial epithelium. Consequently, the dose received by basal or secretory cell nuclei at a given depth in bronchial epithelium depends on the relative distribution of radon progeny in these three compartments. At present, basal and secretory cells are commonly considered as the principal target cells for alpha particle irradiation[29]. The location and volumetric densities of these cells[32] were used in the present work to evaluate cell-specific doses. At low doses of alpha particles, only small fraction of the irradiated cell population is actually intersected by alpha particle tracks. Those cells traversed, however, receive a relatively high cellular dose

Based on the parameters of activity size distribution of ^{214}Bi and^{214}Po (Table 1), the deposition fraction of Radon progeny activity has been calculated using the deposition model of International Commission on Radiological Protection[38]. The total deposition fraction through the human lung was found to be 98% for unattached fraction and 22% for attached fraction.

Figure 4 shows the variation of dose with depth into the bronchial epithelium of airway generation 6 for ^{214}Po alpha particles emitted either from the top of 11 μm thick gel and sol layer, or from the top of the 6 μm thick sol layer or from the interface between the sol layer and the underlying epithelium (curves 1-3). Corresponding calculations for ^{214}Po alpha particles nuclides within epithelial tissue refer either to a uniform distribution of nuclides across the epithelium or to

a nuclide distribution decreasing in a linear fashion with increasing depth in tissue (curves 4-5). Curves 1-3 show that the dose decreases rapidly with increasing depth. In contrast, however, the same number of alpha particles that decay from radon progeny located in the epithelium (linear and uniform case) produced a relatively constant dose throughout the tissue (curves 4-5).
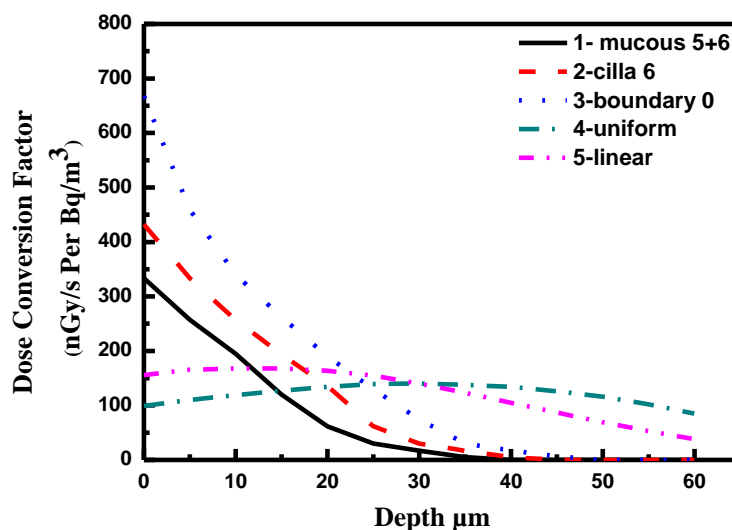

Fig. 4. Dose conversion factor as functions of depth in bronchial epithelium of airway generation 6 for ^{214}Po alpha particles emitted. (1) From the top of the 11 μm thick mucus sol and gel layer, (2) From the top of the 6 μm thick sol layer, (3) From the interface between the sol layer and epithelial tissue, (4) From nuclide distributed uniformly within the bronchial epithelium and (5) From a nuclide distribution decreasing linearly with depth in epithelial tissue.

While present dose calculations generally assume equal densities of basal and secretory cells in bronchial tissue[29], the actually measured volumetric densities for these target cells at varying depth[32] were used here. Such cell-specific depth dose conversion factors could be obtained by multiplying the above computed depth-dose distribution for a uniform distribution of cell nuclei by respective depth-density distributions.

Figure 5 displays the distribution of doses in secretory and basal cells for ^{214}Po alpha particles in airway generation 6. Considering their relative frequencies at a given depth in tissue, the secretory cell doses are relatively homogeneous. The depth-dose distribution for basal cell nuclei, however, has a distinct maximum at greater depth in tissue, where radiation doses were much smaller than for the shallower lying secretory cells. Consequently, the maximum frequency of basal cell doses was shifted to the lower dose range. Figure 5 shows that the mean dose was 44 nGy for basal cells and 112 nGy for secretory cells.
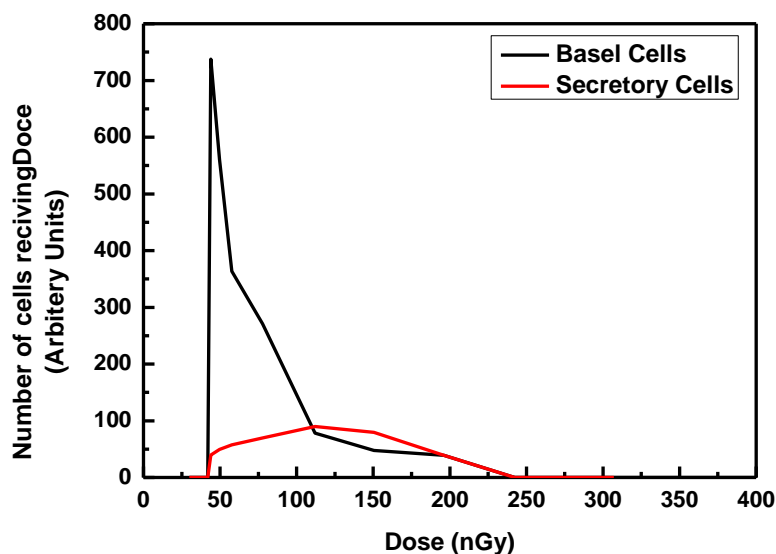
Fig. 5. Distribution of doses in secretory and basal cells for ^{214}Po alpha particles in airway generation 6.

Conclusion

The attached size distributions of ^{214}Bi progeny could be described by unimodal log normal distribution. Most of the attached activities were associated with the accumulation mode. The AMAD of this mode for ^{214}Bi was determined to be 350 nm with GSD□of 3. The GSD of unattached size distributions for ^{214}Po is 1.29 with AMTD of 1.25 nm.

The specific location of radon progeny within the mucous sheath affects the dose to epithelial cells: ^{214}Po alpha particles deposited on bronchial airways are emitted from the top of gel layer, or from the top of sol layer or from the interface between the sol layer and the underlying epithelium. Two additional assumptions have been made when the activity is distributed within the epithelium: A uniform distribution of nuclides across the epithelium or a linear distribution. These simulations suggest that the relative frequencies of the various alpha particle sources may appreciably affect the related cellular dose estimates.

References

1. **Nero, Jr A.V.,** Radon and its decay products in indoor air: an overview. In: Nazaroff WW, Nero, Jr A.V., editors. Radon and its decay products in indoor air. New York: John Wiley & Sons; p. 1–53 (1988).

2. **Vaupotič, J. and Kobal, I.,** Effective doses in schools based on nano-size radon progeny aerosols, *Atmospheric Environment*, **40**, 749-750 (2006).

3. **Dankelmann, V., Reineking, A. and Porstendörfer, J.**, Determination of neutralisation rates of ^{218}Po ions in air. *Radiat. Prot. Dosim.* **94**, 353–7 (2001).

4. **Becker, K. H., Reineking, A., Scheibel, H. G. and Porstendorfer, J.,** Radon daughter activity size distributions, *Radiat. Prot. Dos* in **7**, 147-150 (1984).

5. **Hopke, P. K., Ramamurthi, M. and Li, C. S.**, Measurement of the size distributions of radon progeny in indoor air, In: *"Aerosol: Science, Industry, Health and Environment"*, Masuda, S. and Takashi, K., (Ed.), 2, Pergamon Press, Ltd, Oxford, pp.842-847 (1990).

6. **Reineking, A., Scheibel, H. G., Hussin, A., Becker, K. H. and Porstendorfer, J.,** Measurements of stage efficiency functions including inter-stage losses for Sierra and Berner impactor and evaluation of data by modified simplex method. *J. Aeros. Sci.* **15**, 346 (1984).

7. **Reineking, A., Buttenweck, G., Kesten, J. and Porstendorfer, J.,** Thoron gas concentration and aerosol characteristics of thoron decay products, *Radiat. Prot. Dosim.* **45**, 353-356 (1992).

8. **Reineking, A., Knutson, E. A., George, A. C., Solomon, S. B., Kesten, J., Butterweck, G. and Porstendörfer, J.,** Size distribution of unattached and aerosol-attached short-lived radon decay products: Some results of intercomparison measurements, *Radiat. Prot. Dosim.* **56**, 113-118 (1994).

9. **Mohammed, A.,** Activity size distribution of short-lived radon progeny in indoor air, *Radiat. Prot. Dosim*. **86**(2), 139–145 (1999).

10. **Georges, M.**, *Risk assessment of exposure to Radon decay products final report*, Commission of the European Communities C.E.C. (2000).

11. **Huet, C., Tymen, G. and Boulaud, D.**, Size distribution, equilibrium ratio and unattached fraction of radon decay products under typical indoor domestic conditions, *The Science of the Total Environment*, **272**, 97–103 (2001).

12. **Porstendörfer, J.** Influence of Physical Parameters on Doses from Radon Exposures, *Int. Congr. Ser.* **1225**, 149-160 (2002).

13. **Vaupotič, J. and Kobal, I.,** Short communication radon doses based on alpha spectrometry, *Acta Chim. Slov*. **51**, 159−168 (2004).

14. **EL-Hussein, A.,** Thoron concentration and size distribution of unattached and attached fraction in open air and estimation of equivalent dose. *International Journal of Pure and Applied Physics (IJPAP),* **1** (1), 91–105 (2005).

15. **Yamasaki, K., Oki, Y., Yamada, Y., Tokonami, S. and Iida, T.** Optimization of Measuring Methods on Size Distribution of Naturally Occurring Radioactive Aerosols. *Int. Congr. Ser.* **1276**, 297-298 (2005).

16. **Kranrod, C., Tokonami, S., Ishikawa, T., Sorimachi, A., Janik, M., Shingaki, R., Furukawa, M., Chanyotha, S. and Chankow, N.**, Mitigation of the effective dose of

radon decay products through the use of an air cleaner in a dwelling in Okinawa, Japan, *Applied Radiation and Isotopes,* **67**, 1127–1132 (2009).

17. **Mishra, R., Mayya, Y. S. and Kushwaha, H. S.**, Measurement of 220Rn/222Rn progeny deposition velocities on surfaces and their comparison with theoretical models, *Aerosol Science,* **40**, 1–15 (2009).

18. **James, A. C., Cross, F. T., Durham, J. S., Briant, J. K., Gehr, P., Masse, R., Cuddihy, R. G. and Birchall, A.,** Dosimetry model for bronchial and extrathoracic tissues of the respiratory tract. *Radiat. Prot. Dosim.* **37**, 221-230 (1991).

19. **Mohammed. A. and El-Hussein, A.,** Comparison of outdoor activity size distributions of ^{220}Rn and ^{222}Rn progeny, *Applied Radiation and Isotopes*, **62**, 955–959 (2005).

20. **Butterweck-Dempewolf, G., Shuler, Ch. and Vezzu, G.**, Size Distribution of the unattached fraction of radon progeny. *European Conference on Protection* (1997).

21. **Reineking, A., Porstendorfer, J., Butterweck, G. and Kesten, J.**, Continuous measurements of free and aerosol-bund radon and thoron daughter products in air, *Proc. Coll. Measurements of Radon and Radon Daughter Products.* Koln: TeVRheinland, FS-91-56-T. 94-102 (1991).

22. **Hofmann, W., Steinhäusler, F. and Pohl, E.**, Dose calculation for the respiratory tract from inhaled natural radioactive nuclides as a function of age part 1. compartments deposition, retention, and resulting dose. *Health Phys.* **37**, 517-523 (1979).

23. **Hofamnn, W., Martonen, T. B. and Menache, M. G.**, *Radiation Protection Dosimetry*, **30**, 245-259 (1990).

24. **Hofmann, W., Nosterer, M., Menache, M. G., Crawford-Brown, D. J., Caswell, R. S. and Coyne, J. J.,** Microdosimetry and cellular radiation effects of radon progeny in human bronchial airway. *Radiat. Prot. Dosim.* **52**, 381-385 (1994) .

25. **El-Hussein, A., Ahmed, A. A. and Mohammed, A.** Radiation dose to the human respiratory tract from inhalation of radon-222 and its progeny. *Applied Radiat. Isot.* **7**, 783 (1997).

26. **Winkler-Heil and Hofmann, W.** Comparison of modeling concepts for radon progeny lung dosimetry. In: High level of natural radiation and radon areas: radiation dose and health effects. *Proceeding of the Fifth International Conference on High Levels Health Levels of Natural Radiation and Radon Areas: Dose and Health Effects*. Sep. 4-7th, Munich. Excerpts Medica.International Congress Series **1225** (2000).

27. **Marsh, W. and Brichall, A.,** Sensitivity analysis of the weighted equivalent lung dose per unit exposure from radon progeny. *Radiat. Prot. Dosim.* **87** (3), 167-178 (2000).

28. **Marsh, W., Brichall, A., Butterweck, G., Dorrian, M.-D., Huet, C., Ortega, X., Reinking, A. Tymen, G., Schuler, Ch., Vargas, A. and Vezzu, G.,** Wendt, J. Uncertainty analysis of the weighted equivalent lung dose per unit exposure to radon progeny in the home. *Radiat. Prot. Dosim.* **102** (3), 229-248 (2002).

29. **National Research Council (NRC),** "*Comparative Dosimetry of Radon in Mines and Homes*". National Academy Press, Washington, DC (1991).

30. **Harly, N. H.** *Cycling Cells Radon Res. Notes*, **15**, 9-10 (1995).

31. **Baldwin, F., Hovey, A., McEwen, T. and Oconnr, R.**, Unruh, H. and Bowden, D. H. Surface to nuclear in human bronchial epithelium. Relationship to penetration by Rn daughters. *Health Phys*. **60**, 155-162 (1991).

32. **Mercer, R. R., Russell, M. L. and Grapo, J. D.,** Radon dosimetry based on the depth distribution of nuclei in human and rat lungs. *Health Phys.* **61**(1), 117-130 (1991).

33. **Lurzer, C.,** Uber die Bestimmung von Multimodalen Grossenverteilungen Atmospharischer Aerosole, Mittels unterdrckkaskaden impaktoren, Dissertation, Wien, Austria (1980).

34. **William, C. Hinds.** "*Aerosol Technology. Properties, Behavior, and Measurement of Airborne Particles*", 2nd ed., Wiley, New York (1999).

35. **Ruffle, M. P.**, The geometrical efficiency of a parallel disc-source and detector system, *Nucl. Instr. Meth*. **52**, 354-356 (1967).

36. **Wicke, A.**, UntersuchungenzurFrage Der NaturlichenRadioactivitat der Luft in Wohn undAufenthaltsraumen. *Ph.D. Thesis*, University Gissen, Germany (1979).

37. **Ahmed, A. A.,** Untersuchungen zur Aerosol Deposition an Oberflachen, *Ph.D. Thesis,* University Giessen, Germany (1979).

38. **International Commission on Radiological Protection (ICRP)**, Human Respiratory Tract Model for Radiological Protection.Pergamon Press, Oxford, ICRP Publication 66 (1994).

الجرعات الإشعاعيـة خلال رئة الانسان الناتجـة مـن استنشـاق نـواتج تحلل الرادون٢٢٢

عامر محمد محمد ، مصطفى لطفى عبدالهادى ، منى مصطفى محمود, مصطفى يونس عبدالفتاح و محمود محمد اسماعيل*

قسم الفيزيـاء ـ كلية العلوم ـ جامعة المنيا ـ المنيا و*قسـم الفيزيـاء ـ كلية العلوم ـ جامعة الازهر ــ القاهره ــ مصر.

حسـاب الجرعـات المترسـبه او الممتصـه مـن الطاقـات المؤينـه المنبعثـه مـن الاشعاعات الناتجه من المواد المشعه يصعب تنفيذه عمليا. فى هذا البحث نستخدم النماذج النظريه لتقدير هذه الجرعات خاصة في رئة الانسان. هذه النماذج النظريه تحتاج إلـي البـارامترات الخاصـه بـالتوزيع الحجمـي للعناصـر المشـعه مثـل نظـائر الرادون. تم في هذا البحث حساب هذه البارمترات للجزء الحر والمرتبط من نظائر الرادون (البيزمث ٢١٤ والبولونيوم ٢١٤) وقد تم القياس في امـاكن الاقامـه المغلقه بجامعة المنيا ـ مدينة المنيا ـ جمهورية مصر العربيه.وقد تم قياس الجزء المرتبط لوليدات الرادون باستخدام جهـاز الامبـاكتور منخفض الضغط فـي تجميع العينـات وتحليلها باستخدام طيف اشعة جاما بينمـا تم قياس الجزء الحر باستخدام مصدر طاقة الانتشار٫ التجميع والقياس باستخدام طيف جسيمات الفا. وقد اتضح من النتائج المستخلصه أن معظم حجم الجسيمات الحره متواجد في النطاق التراكمي للجسيمات (من ١٠٠ إلى ٢٠٠٠ نانو متر) وهو النطاق الاخطر بسبب طول زمن بقائه في الهواء مما يزيد فترة التعرض للمقيمين فى المناطق المغلقه. وتم حساب متوسط قطر الجسيمات وقد وجد انه ٣٥٠ نانومتر بالنسبه إلي البيزمث ٢١٤. امـا في حالـة الجزء الحر وجد ان متوسط القطر في حدود ١٬٢٩ نـانومتر لعنصر البولونيوم ٢١٤. وقد تم استخدام الطرق التحليليه لتقدير جزء الطاقه المترسب من جسيمات الالفـا المنبعثـه مـن عنصـر البولونيـوم ٢١٤ عنـد مسـتويات مختلفـه مـن الشـعب الهوائيه ٫ويكون حساب الجرعه الاشعاعيه من خلال سريان جسيمات الالفا داخل الانسجه أو في الهواء والانسجه معا. وقد لوحظ انه مع ازديـاد العمق فى الشـعب الهوائيه نقص في توزيع الجرعه.